

JP2.17

A STUDY OF CLOUD TOP MICROPHYSICAL CHARACTERISTICS IN HIGH PLAINS THUNDERSTORMS

William C. Straka III⁺, Daniel T. Lindsey[#], Andrew K. Heidinger^{*}

⁺ Space Science and Engineering Center, University of Wisconsin at Madison, Madison, WI

[#] Regional and Mesoscale Meteorology Branch, NOAA/NESDIS, Ft. Collins, CO

^{*}Office of Research and Applications, NOAA/NESDIS, Madison, WI

1. INTRODUCTION

Satellite observations of thunderstorms have been documented since the advent of the Geostationary Operational Environmental Satellites (GOES) in the 1970's. There have been several studies on both the near storm environment (Purdum 1976; Weaver and Purdom 1995; Bikos et al. 2002) and storm-top characteristics of severe storms (Heymsfield et al., 1983; McCann, 1983; Adler and Mack, 1986; Setvák and Doswell, 1991).

Since GOES-8, launched in 1994, the 3.9 μm channel has been available for daytime, satellite-observed radiances with both thermal and reflected solar components. This study was motivated by several reasons. The first reason is the interest in the microphysical aspects of severe thunderstorms. The next reason is that it is thought that larger water particles can travel up to the top of thunderstorms in more intense updrafts. This would be shown by a significant difference in effective radii in the core of the storm, as larger supercooled water drops would be surrounded by smaller ice particles. Finally, it has been shown that some thunderstorm tops have enhanced solar reflectivity in the shortwave infrared portion of the spectrum, which may be due to differences in the microphysical structure at cloud top (Lindsey et al., 2006). In particular, these highly reflective storm tops are likely associated with small ice crystals within the thunderstorm anvils.

This study will use methods developed for the GOES Surface and Insolation Program (GSIP), to estimate the cloud top effective radius and total column optical depth using GOES imager data. The goal of this study is to look at the changes in cloud top effective radius and optical depth during thunderstorm lifecycles in the High Plains of the United States. In addition, we will compare the GSIP effective radius retrieval with an experimental effective radius retrieval for optically thick, convectively generated ice clouds, in which the scattering properties of droplets are assumed. We provide a case study in which storms have observed diurnal changes in the 3.9 μm reflectivity and large variations in ice crystal effective radius.

2. CASE STUDY DESCRIPTION

A single day, 6 June 2005, was used for this particular case study. We chose this date because of the presence of thunderstorm activity in the area that both GOES-10 and GOES-12 observe and are not on the limb of both imagers. Convection initiated in response to a slow-moving low pressure system situated in central Wyoming. There were storms occurring behind the occluded front in northwestern Montana and in northern Utah. As the day progressed, the cold front associated with the low triggered storms along the Front Range of Colorado. The northward movement of these storms was in response to 850-500 mb wind, which was to the north around the low. The movement of the low was in response to the jet stream around a deep low centered off the Washington coast.

Hourly data from 1500 UTC to 2345 UTC were taken from both GOES-10 and GOES-12 to perform the analysis. This allowed for approximately 10 hours of observations from both satellites, and for thunderstorm development and maturity to be observed. The

*Corresponding author address: W.C. Straka III, Space Science and Engineering Center, Cooperative Institute for Meteorological Satellite Studies, 1225 West Dayton Street, Madison, WI 53706; Fax: (608) 262-5974; e-mail: wstraka@ssec.wisc.edu

main thunderstorm development on this day took place in eastern Wyoming and western North Dakota.

For the comparative study between the GSIP and CIRA effective radius retrieval, data from 21N to 54N were taken. This allows us to utilize more hourly data, since full disk scans from GOES are only performed 4 times a day. Limits on the longitude were set to take into account the limb of the imager. For GOES-10, the limits were set between -125E and -95E longitude. For GOES-12, the limits were set at -110E to -68E. Both effective radii datasets were quality controlled.

3. DIURNAL CHANGES

The following section focuses on the diurnal cycle of the storms on 6 June 2005. We will compare the changes between GOES-10 and GOES-12, and focus on the storms that occurred in eastern Wyoming.

a. GOES-10

At 1500 UTC (Figure 1) the initial convection observed for this study is easily seen in northeastern Wyoming by the high effective radii near the updraft region of the convection (greater than 25 microns). GSIP classifies this region as supercooled water and opaque ice cloud. This is indicative of the cool water drops and ice particles in the convective top region. The cloud type of “overlapped cirrus” and “non overlapping cirrus” near this region, shown by the lower cloud top effective radii near this cell, is indicative of the anvil cloud, which tends to be shown as areas less than or equal to 25 microns.

By 1600 UTC, the area described above has reduced in effective radii and begins to be classified as “non overlapped cirrus cloud”, implying that it is turning into just the remaining anvil cloud. However, to the south, another line of storms develops briefly along a trough that was traveling east with a low pressure moving from western Wyoming. The storms that developed in east-central Colorado were pulled along as the low moved to the northeast. By

1900 UTC, another set of storms forms in roughly the same location as the first. The first signs of clouds developing are pixels of low effective radii (10 microns or less), which are liquid water clouds. These then form into regions of higher effective radii super-cooled water clouds. Finally, as these clouds glaciate and form ice crystals, the cloud top particle size over the convective region decreases. The smaller particles are then blown off into the anvil region. However, in the convective regions, larger (greater than 25 microns) particles still exist, as evidenced by the areas of higher effective radius in Colorado and Montana.

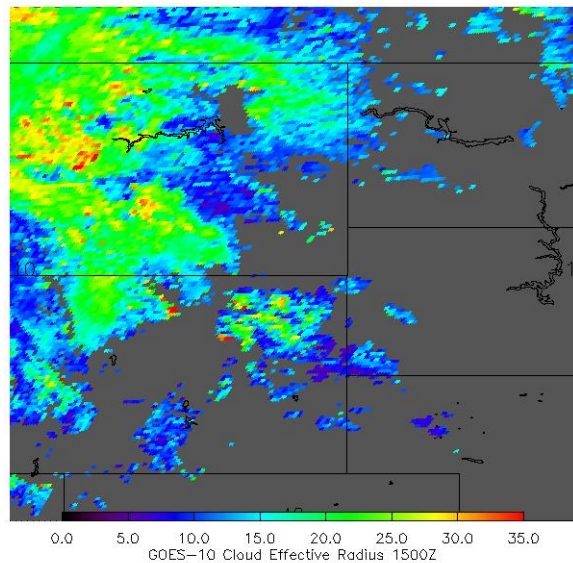


Figure 1. Effective radius for 1500 UTC from GOES-10 as calculated by GSIP

Optical depth increases as the cloud becomes more convective. The anvil is optically thinner since there is not as much cloud present. This is due, in part, to the smaller particles are blown away from the main convection. This can be seen in Figure 2, which is the effective radius at 2300 UTC. You can see that the anvils in southeastern South Dakota have smaller effective radii (around 20 microns). In addition, the convective cirrus, or the anvil, have smaller effective radii than the cirrus not associated with convection, such as the cirrus over western Montana (effective radii of around 10 -15 microns).

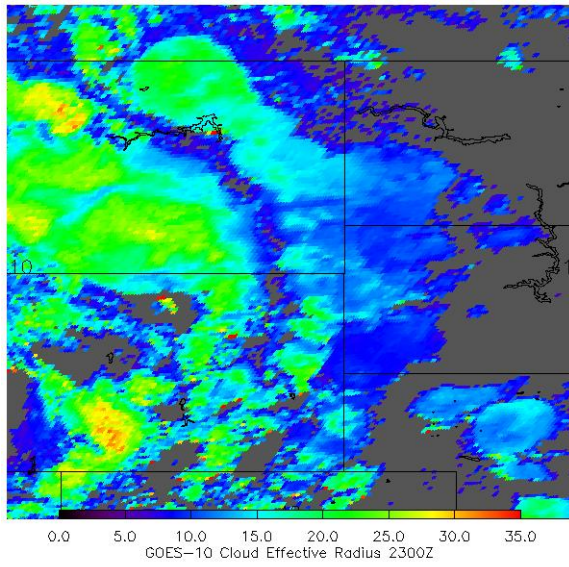


Figure 2. Same as Figure 1, except for 2300 UTC

b. GOES-12

The effective radii data from GOES-12 is very similar to that described above for GOES-10. However the one big difference is that the effective radii calculated for the GOES-12 imager is smaller for a given region. This is because of the differences in the satellite viewing angle as well as the differences in the lookup tables and imager between the two satellites.

4. EFFECTIVE RADIUS RETRIEVAL COMPARISON

A new ice cloud effective radius retrieval has been developed at the Cooperative Institute for Research of the Atmosphere (CIRA). It will be compared with the GSIP retrieval on 6 June 2005 for the simple purpose of documenting any biases which exist between the two methods.

To produce CIRA's lookup tables, an observational operator, which includes a forward radiative transfer model (SHDOM), was run over a wide range of clouds and satellite viewing angles. An optically thick ice cloud was placed in the model domain, and ice crystal effective radius was varied between 7 - 52 μm . To obtain

the optical properties associated with these ice clouds, scattering tables provided by Yang et al. (2003) were used to obtain the single-scatter albedo, extinction, and scattering phase function. The phase function was represented by 2500 Legendre polynomials. Droxtals were assumed for all clouds. With the lookup tables in place, clouds whose 10.7 μm brightness temperature is colder than -40°C are chosen, and 3.9 μm reflectivity is calculated. This value is used along with solar zenith angle and scattering angle to obtain the proper effective radius from the lookup tables.

Fig. 3 is a scatterplot of the comparisons between GSIP and the CIRA retrieval from 6 June 2005, for GOES-12. The best-fit line has a slope of 0.38, and the R-squared value is 0.48. This means that CIRA has a significant high bias compared to GSIP, and a good deal of variance exists, especially with the larger values. Looking at the diurnal trend of this comparison, the high bias exists at all times, but the R-squared values become quite low earlier in the day. This suggests that either a) the retrievals are more similar with active convective clouds in the afternoon, or b) there is a significant difference in the scattering geometry between morning and afternoon with the two retrieval methods.

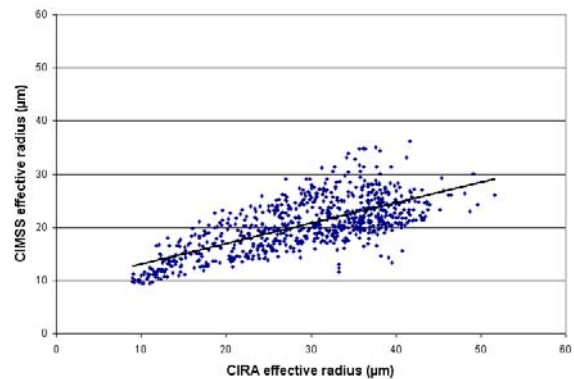


Figure 3. Effective radius retrievals from ice clouds on 6 June 2005 from CIMSS (GSIP) and CIRA. The black line is a linear best-fit.

Fig. 4 is similar to Fig. 3, except for GOES-10. Best-fit line slope is 0.46, and the R-squared value is 0.68, both of which are slightly better than with GOES-12. These differences could be related to the different viewing geometry, but

more likely they are simply due to a different set of clouds being sampled. A similar diurnal trend also exists with GOES-10, i.e., the retrievals become increasingly different earlier in the day.

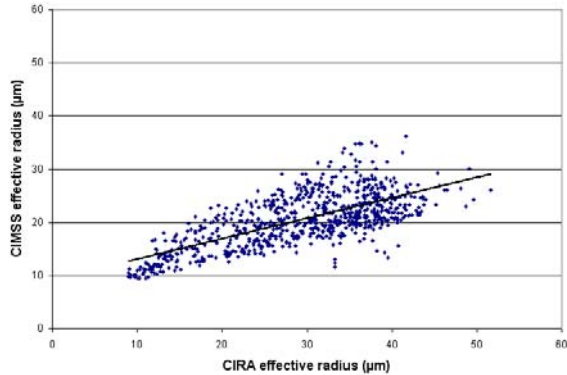


Figure 4. Same as Fig. 2, except for GOES-10.

5. CONCLUSIONS

This study has shown that the effective radius derived on an operational basis can capture the cycle of a storm. This includes the initiation (low effective radii coupled with a liquid water cloud type), intensification (higher effective radii coupled with super-cooled water), glaciation (a reduction in effective radii coupled with a glaciated cloud type), and the anvil development outside of the convective region (lower effective radii coupled with a non-overlapping cirrus cloud type). The effective radii that are present in the intensification stage are relative to the initial effective radius. However, when comparing a vigorous towering cumulus cloud to a less vigorous cloud of similar height, the effective radii would be smaller. This is likely because the drops have had more time to grow in the weaker updrafts (Rosenfield and Lensky 1998). If you look at the individual storms themselves, you often find areas of higher effective radii embedded in the anvil shield, near the region of convective updraft. In addition, GSIP categorizes these areas as areas of supercooled water. While these two factors do not necessarily mean that supercooled water is present, since supercooled water droplets do not necessarily have larger effective radii than the surrounding anvil, it is a possible indicator. Areas of high effective radius

are often spotted in clouds where the anvil is just at or slightly below cloud top temperatures of -40°C . These high effective radii were typically observed as storms began to reach their mature stage. Once these storms became mature they reached cloud top temperatures less than -50°C . Thus, these features disappeared. Thus, this may be a sign of the supercooled water poking out from the top of the anvil shield, and an indicator of where the more updraft is located, during the development to mature stages of a thunderstorm.

We have also compared two separate and unique algorithms used to calculate effective radius using the $3.9\ \mu\text{m}$ channel. It was found that the algorithm used in GSIP produced lower effective radii over the course of the day. The diurnal trend of this comparison showed that there was a high bias that existed no matter what time of the day. However, the R-squared values are lower earlier in the day compared to later in the day. This suggests that the retrievals are more similar with active convective clouds in the afternoon, or there is a significant difference in the scattering geometry between morning and afternoon with the two retrieval methods. This is something that will be investigated as these algorithms continue to be developed. It is quite difficult to say which method is "better", since many assumptions about ice scattering are necessary. Both provide information about diurnal trends in effective radius, which is the more valuable piece of information.

One problem this and other studies of effective radius show is that, currently the solar component of the $3.9\ \mu\text{m}$ channel is used to calculate the cloud top effective radii and other cloud microphysical properties. This means that we cannot determine the microphysical properties of clouds at night. This is a problem as interesting phenomenon, such as MCSs, occur at night. It is the hope that with different channels on platforms such as SEVIRI, on the Meteosat Second Generation satellites, and the ABI, which will be incorporated on the GOES-R satellite, that algorithms can be developed to perform a more comprehensive study of the diurnal effect of cloud top effective radius.

6. REFERENCES

Adler, R. F., and R. A. Mack, 1986: Thunderstorm cloud top dynamics as inferred from satellite observations and a cloud top parcel model. *J. Atmos. Sci.*, 43, 1945–1960.

Bikos, D. E., J. F. Weaver, and B. C. Motta, 2002: A satellite perspective of the 3 May 1999 Great Plains Tornado Outbreak within Oklahoma. *Wea. Forecasting.*, 17, 635–646.

Heymsfield, G. M., R. H. Blackmer Jr., and S. Schotz, 1983: Upper-level structure of Oklahoma tornadic storms on 2 May 1979. I: Radar and satellite observations. *J. Atmos. Sci.*, 40, 1740–1755.

Lindsey, D.T., D. W. Hillger, L. Grasso, J. A. Knaff, and J. F. Dostalek, 2006: GOES Climatology and Analysis of Thunderstorms with Enhanced 3.9 μm Reflectivity. *Mon. Wea. Rev.*, in press.

McCann, D. W., 1983: The enhanced-V: A satellite observable severe storm signature. *Mon. Wea. Rev.*, 111, 887–894.

Purdum, J. F. W., 1976: Some uses of high-resolution GOES imagery. *Mon. Wea. Rev.*, 104, 1474–1483.

Rosenfeld, D. and I. M. Lensky, 1998: Satellite-based insights into precipitation formation processes in continental and maritime convective clouds. *Bull. Amer. Meteor. Soc.*, 79, 2457–2476.

Setvák, M., and C. A. Doswell III, 1991: The AVHRR channel 3 cloud top reflectivity of convective storms. *Mon. Wea. Rev.*, 119, 841–847.

Weaver, J. F., and D. T. Lindsey, 2004: Some Frequently Overlooked Severe Thunderstorm Characteristics Observed on GOES Imagery: A Topic for Future Research. *Mon. Wea. Rev.*, 132, 6, 1529–1533.

Weaver, J. F., and J. F. W. Purdom, 1995: An interesting mesoscale storm– environment

interaction observed just prior to changes in severe storm behavior. *Wea. Forecasting.*, 10, 449–453.

Yang, P., B. A. Baum, A. J. Heymsfield, Y. X. Hu, H. L. Huang, S. C. Tsay, and S. Ackerman, 2003: The single-scattering properties of droxtals. *J. Quant. Spectr. and Rad. Trans.*, 79, 1159–1169.